

Morphological instability of a terrace edge during step-flow growth

G. S. Bales and A. Zangwill

School of Physics, Georgia Institute of Technology, Atlanta, Georgia 30332-0430

(Received 15 November 1989)

We consider the possibility that monoatomic terrace edges undergo a morphological instability during epitaxial *step-flow* growth. A linear stability analysis predicts that such an instability *can* occur, but only when the energy barriers to adatom attachment to steps *differ* for adatoms that approach a step from *opposite* directions. The instability is diffusional in origin and manifests itself as a distinct waviness or meandering of the terrace edges as they propagate across the crystal. Our results, presented in the form of a morphological phase diagram, show that single-crystal growth on a vicinal surface can pass from stable step flow to unstable step flow to two-dimensional island nucleation and spreading as one increases the incident flux in a molecular-beam-epitaxy experiment at elevated temperature. The instability we predict should be readily distinguishable from simple thermal fluctuations.

I. INTRODUCTION

The ability to grow single-crystal materials with essentially monolayer compositional control is one of the central features of modern crystal-growth techniques such as molecular-beam epitaxy (MBE) and organometallic vapor-phase epitaxy (OMVPE).¹ Indeed, the fabrication of one-dimensional superlattice structures has become sufficiently commonplace that forefront research now focuses on the creation of novel epitaxial architectures, e.g., quantum wires, by judicious manipulation of the deposition process.² These recent efforts have rekindled interest in the fundamental physics of single-crystal growth itself, with particular emphasis on *layer growth*.³ Most of this work is experimental, ranging from the careful measurement and interpretation of anisotropic macroscopic growth rates⁴ to atomic resolution scanning tunneling microscopy of thin films interrupted during growth by a quench.⁵

For the case of MBE, analyses of reflection high-energy electron diffraction (RHEED) data collected *in situ* have proven particularly valuable.⁶ Distinct oscillations in RHEED intensities observed during growth commonly are interpreted as indicative of layer growth by the nucleation and spread of two-dimensional islands on a (nominally) flat substrate.⁷ The disappearance of such oscillations is ascribed either to the onset of multilayer surface roughness (if one waits long enough) or to a transition to a different mode of growth (if one raises the substrate temperature). The aforementioned kinetic roughening effect is rather poorly understood at present. On the other hand, so-called *step flow* has long been recognized as the alternative to two-dimensional nucleation as a layer-growth mechanism.³

Epitaxial growth on a vicinal surface can provide an excellent example of step flow. Such a surface consists of broad terraces (of mean width l) separated by monoatomic steps (Fig. 1). In the simplest case, a flux F of atoms impinges upon the solid, chemisorption occurs, and adatoms diffuse (D_s) across the terraces. Some atoms desorb

back into the gas phase after a characteristic time τ while the remainder eventually reach a step. Arrhenius-type rate constants k_+ and k_- characterize the probability that newly arrived atoms actually bond to the upper and lower terrace edges, respectively.⁸ Such attachments obviously advance the terrace edge perpendicular to itself so that, in steady state, all steps flow across the surface. Growth proceeds monolayer by monolayer.

High⁶ and low⁹-energy electron microscopy provide direct visual evidence that this simple scenario is largely correct. For semiconductors, step flow is essential to the growth of tilted-layer superlattices¹⁰ and certain quantum wire geometries,¹¹ while for metals, physical arguments directly based upon the step-flow picture have helped determine superlattice growth parameters.¹² In all these cases, (relatively) high-temperature and low deposition flux must be used in order to avoid two-dimensional nucleation on the terraces.^{7,13}

Step flow was treated quantitatively long ago in a seminal paper by Burton, Cabrera, and Frank¹⁴ (BCF). Their model addresses the physical situation outlined above with the additional assumption that every terrace edge acts as a perfect sink, i.e., the kinetics of step attachment

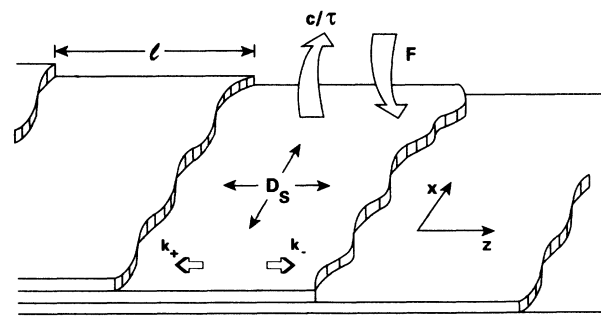


FIG. 1. Schematic view of a vicinal surface during step-flow growth.

are infinitely fast. This is equivalent to the assumption that the adatom concentration in the immediate vicinity of each step attains its equilibrium value. BCF considered two characteristic topologies in detail: a sequence of equidistant, straight, parallel steps, and loops or spirals of steps characterized by a local radius of curvature. The main result of their calculation was an expression for the velocity of step propagation and a corresponding prediction for the macroscopic growth rate.

In the years since its introduction, the BCF model has been generalized to take account of many factors thought to be important in real layer growth. In particular, the assumption of local equilibrium at the steps has been relaxed¹⁵ with particular attention to the case ($k_+ \neq k_-$) where the energy barriers encountered by adatoms that approach a step from opposite directions are not equal.¹⁶ A good discussion of this problem (and the BCF literature in general) can be found in a recent article by Ghez and Iyer.¹⁷ Interestingly, the straight step and spiral step topologies continue to dominate discussion and comparison with experiment.^{18,19} This is true despite the fact that microscopy often reveals that step patterns can be quite wavy.^{6,8,20,21} In some cases their irregularity exhibits a strong dependence on crystallographic orientation.^{22,23}

The origin of wavy or meandering steps usually has been attributed to the nature of step sources, impurity capture, surface defects, or thermal fluctuations. In fact, $T=0$ is the so-called *roughening temperature* T_R for an isolated step. This means that, for any $T > T_R$, an initially straight step of length L will wander until, in equilibrium, its end points become separated (in the direction perpendicular to the step) by a distance $\sim \sqrt{L}$.^{24,25} Within the context of step flow, the standard BCF treatment actually applies only to a "rough" step because it presumes a linear kink density of sufficient magnitude that every point along the step length is a potential adatom capture site. Voronkov²⁶ has examined this question in more detail and concludes that a sort of "random-step waviness" can result during growth. This is undoubtedly the origin of some observations of step wandering, particularly since, for a real vicinal surface, the magnitude of the step roughening temperature depends on both the mean terrace width and the step crystallography.²⁷

Nonetheless, many experiments reveal step roughness of a decidedly nonrandom nature.^{6,21} The purpose of the present work is to point out that certain wavy step patterns may have a very different, intrinsic origin. In particular, we propose an explanation based upon the fact that a growth front propagating at $T > T_R$ under conditions of diffusion control can exhibit an intrinsic morphological instability.²⁸ In certain circumstances to be detailed below, this instability can manifest itself during step flow to yield terrace edge waviness of a very characteristic form. In the extreme case, we obtain "surface dendrites" (of monolayer height) that propagate across the surface of an otherwise perfect single crystal.

Our discussion is organized as follows. In Sec. II we review the BCF model of step flow and provide a qualitative argument which establishes the conditions under which morphological stability can be lost. Section III is

devoted to a linear stability analysis of the (suitably generalized) BCF equation which makes the qualitative arguments mathematically precise. Our final results are presented in the form of a morphological phase diagram. Section IV contains a discussion of some of the limitations of our analysis, the nature of morphological evolution in the nonlinear regime, and some qualitative guides to the experimentalist. We summarize our results in Sec. V.

II. QUALITATIVE DISCUSSION

Our analysis of morphological stability during step flow employs the uniform vicinal surface topology of Fig. 1. Following Ref. 14, we consider only homoepitaxy and a ballistic flux of atoms, i.e., the MBE case.²⁹ The assumption that all steps propagate as atomically rough growth fronts ($T > T_R$) implies that each behaves as a continuous line sink. Moreover, for simplicity, we neglect step-step interactions and ignore any in-plane anisotropy of the surface diffusion constant, the kinetic attachment coefficients and the step surface tension. Given the foregoing, the steady-state concentration of atoms on the terraces $c(\mathbf{r})$ satisfies³⁰

$$D_s \nabla^2 c - \frac{c}{\tau} + F = 0. \quad (1)$$

The problem is completely specified by choice of the boundary conditions for Eq. (1) and the requirement of mass conservation at the step. The latter determines the steady-state velocity of the step as

$$V = \frac{D_s}{\Delta c} \{ \nabla c|_+ - \nabla c|_- \} \cdot \hat{n} = V_+ + V_- . \quad (2)$$

In this expression, Δc is the difference between the areal density of atoms in the solid phase and the corresponding quantity on the terrace immediately adjacent to a step, \hat{n} is a unit normal out of the solid perpendicular to the (monoatomic) step riser, and the plus and minus signs refer, respectively, to points on the terrace displaced from the step by an infinitesimal amount parallel or antiparallel to \hat{n} . Notice that *both* bounding terraces contribute to the flow of a given step.

A qualitative understanding of morphological stability (and instability) during step flow can be gained by reference to Fig. 2. The top panel is a top view of Fig. 1 in the vicinity of a terrace edge where the step "waviness" is taken to be in the form of a small amplitude sinusoid. Isoconcentration lines (dashed) have been drawn for the BCF "perfect sink" boundary condition, i.e., the adatom concentration takes its equilibrium value c_{eq} in the immediate vicinity of the step. The numerical labeling serves to indicate that the adatom concentration $c(\mathbf{r})$ *increases* as one moves away from the step in either direction. Observe that the isoconcentration lines are squeezed together (spread apart) in the immediate vicinity of convex (concave) portions of the curved step.³¹ Thus, relative to a perfectly straight step, the contribution to Eq. (2) from the lower terrace (V_+) is enhanced at point *A* and diminished at point *B*. Conversely, the contribution to the net growth rate from the upper terrace

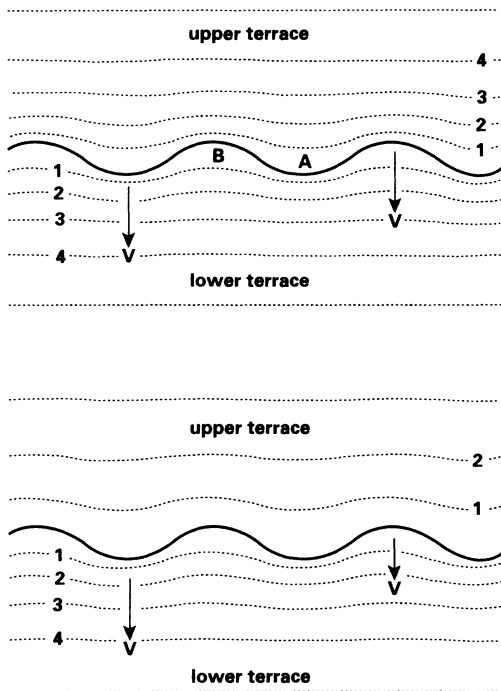


FIG. 2. Top view of Fig. 1 in the vicinity of a perturbed terrace edge. Isoconcentration lines (dashed) qualitatively reflect the solution to Eq. (1) for the case of equal adatom flux toward the step from both bounding terraces (top panel) and for the case when the supply of atoms from the upper terrace is greatly reduced (bottom panel). Note that the rate of advance of different parts of the step is the same in the equal flux case but differs in the unequal flux case.

(V_-) is diminished at point *A* and enhanced at point *B*. Overall, there is no change in the velocity anywhere. The distorted step propagates uniformly without change of shape.

Suppose however, that, by some mechanism, the flux of adatoms that attach to the step from the *upper* terrace is greatly reduced. The isoconcentration lines now appear as indicated in the lower panel of Fig. 2. This change is sufficient to produce a morphological instability in the terrace edge shape. In particular, the amplitude of the perturbation increases spontaneously because the stabilizing effect of the upper terrace no longer compensates for the intrinsically destabilizing influence of the lower terrace. Positive feedback leads to an absolutely unstable situation. It is clear from this argument that stability is lost even if the supply of atoms from the upper terrace is only slightly reduced. Roughly speaking, one requires only that the flux of atoms arriving from the lower terrace exceed the flux of atoms arriving from the upper terrace. Perturbations of any wavelength are predicted to grow without bound.

Of course, an important effect has been omitted from the foregoing. Any perturbation increases the length and hence the total line energy of the step. To reduce this energy cost, a capillary-induced smoothing ensues. One possibility is line diffusion along the terrace edge. How-

ever, under typical MBE conditions, the two-dimensional vapor pressure of the mobile atoms adsorbed on the terraces is likely to be large enough for another smoothing mechanism to dominate: evaporation (detachment) of atoms from convex portions of the step, followed by surface diffusion and condensation (reattachment) onto concave portions of the step. It is possible to regard this current of atoms to and from a curved step as being driven (by Fick's law) by variations in the concentration of adsorbed atoms in equilibrium with the step.³² The latter is described by the Gibbs-Thomson relation,³³

$$c_{\text{eq}}(\mathbf{s}) = c_{\text{eq}}^0 \exp \left[\frac{\Omega \gamma \kappa(\mathbf{s})}{k_B T} \right] = c_{\text{eq}}^0 + \Gamma \kappa(\mathbf{s}) + \dots, \quad (3)$$

where γ is the free energy/(unit length of step), Ω is the atomic area of the solid, $\kappa(\mathbf{s})$ is the curvature of the step at position \mathbf{s} , and k_B is Boltzmann's constant.

The physical processes involved in the relaxation mechanism just described immediately imply that smoothing is very effective for short-wavelength perturbations but increasingly ineffective for perturbations of longer wavelengths. Hence, we anticipate the existence of a *critical wavelength* λ_c . Capillarity guarantees that short-wavelength perturbations ($\lambda < \lambda_c$) decay back to a flat step while the diffusion field bounding the step guarantees that long-wavelength perturbations ($\lambda > \lambda_c$) grow. This is the essence of the so-called Mullins-Sekerka instability.²⁸

From the foregoing, we may anticipate the loss of morphological stability during step flow only when unequal diffusive fluxes impinge upon the steps from adjacent terraces. As it happens, such a flux imbalance is a natural consequence of the phenomenon of asymmetric step attachment kinetics mentioned in the Introduction. This is so because the mere possibility of kinetic barriers to the incorporation of atoms into step kink sites forces one to relax the BCF assumption that steps act as perfect sinks which maintain $c(\mathbf{s}) = c_{\text{eq}}$ at the terrace edges. The appropriate condition emerges from the supposition⁸ that the step velocities V_{\pm} are determined by first-order reaction kinetics:

$$V_{\pm}(\mathbf{s}) = \Omega k_{\pm} [c(\mathbf{s}) - c_{\text{eq}}(\mathbf{s})]_{\pm} \quad (4)$$

characterized by the attachment rate constants k_{\pm} . Eliminating V_{\pm} between Eqs. (2) and (4) and making the (excellent) approximation that $\Delta c \approx \Omega^{-1}$, we obtain

$$D_s \nabla c|_{+} \cdot \hat{n} = k_{+} [c(\mathbf{s}) - c_{\text{eq}}^0 - \Gamma \kappa(\mathbf{s})]_{+} \quad (5)$$

$$-D_s \nabla c|_{-} \cdot \hat{n} = k_{-} [c(\mathbf{s}) - c_{\text{eq}}^0 - \Gamma \kappa(\mathbf{s})]_{-} \quad (6)$$

as the boundary conditions for Eq. (1) at terrace edges.

As noted earlier, k_{\pm} exhibit activated temperature dependences and are not, in general, equal.¹⁶ There is good experimental evidence for the latter assertion. Field-ion microscopy images of surface diffusion on refractory metals directly show atoms "reflecting" from terrace down steps³⁴ while transmission electron microscopy (TEM) images illustrate strongly preferential attachment of Al atoms to $\text{Al}_x\text{Ga}_{1-x}\text{As}$ step risers during the growth of tilted superlattices.³⁵ Thus, consistent with

simple bond breaking arguments, both observations show that $k_- < k_+$, that is, adatom attachment is more likely from the lower terrace. The limit $k_- = 0$ corresponds to the maximally unstable case of complete "blocking" where no atoms join a step from the upper bounding terrace. The BCF equilibrium condition is recovered when $k_{\pm} \rightarrow \infty$.

III. QUANTITATIVE RESULTS

The mathematical machinery we use to study morphology stability is similar to that employed for related problems,²⁸ i.e., a linear stability analysis. For this purpose, it is convenient to introduce a new variable $u(\mathbf{r}) = c(\mathbf{r}) - \tau F$ so that the BCF equation (1) becomes

$$\nabla^2 u - \frac{u}{x_s^2} = 0, \quad (7)$$

where $x_s = \sqrt{D_s \tau}$ is the surface diffusion length. The general solution to this Helmholtz equation is

$$u(x, z) = \sum_k [A_k \sinh(\Lambda_k z) + B_k \cosh(\Lambda_k z)] \times [\sin(kx) + C_k \cos(kx)], \quad (8)$$

where $\Lambda_k = [(1/x_s^2) + k^2]^{1/2}$ and the allowed values of the separation constant k are determined by the boundary conditions. It is clear, for example, that only $k = 0$ is required to obtain the solution $u_0(z)$ appropriate for perfectly straight steps.

To proceed, we perturb the shape of each terrace boundary with a small amplitude sinusoid of a *particular* wave vector k . The position of the m th step then becomes

$$z_m(x) = z_m + \varepsilon \sin(kx). \quad (9)$$

In general, a solution to Eq. (7) which satisfies the conditions (5) and (6) on the curved boundaries defined by Eq. (9) requires many terms in the sum of Eq. (8). However, a two-term solution of the form

$$u(x, z) = u_0(z) + [A_k \sinh(\Lambda_k z) + B_k \cosh(\Lambda_k z)] \varepsilon \sin(kx) \quad (10)$$

can be found if one only requires the result to be correct

to *first order* in the (small) quantity ε . Technically, this involves making a number of approximations including ignoring both the difference between \hat{n} and \hat{z} and non-linear terms which appear in the computation of the curvature in Eqs. (5) and (6).

Finally, we compute the velocity of any step from Eq. (2). Given the preceding equation, this must have the form

$$V(x) = V_0 + \omega(k) \varepsilon \sin(kx), \quad (11)$$

where V_0 is the velocity of a straight step and $\omega(k)$ is a complicated, but known, function of the wave vector k . We now are finished because this velocity also can be computed from the time derivative of Eq. (9) to be

$$V(x) = V_0 + \frac{d\varepsilon}{dt} \sin(kx). \quad (12)$$

Comparing Eqs. (11) and (12), we conclude that $\varepsilon \propto \exp[\omega(k)t]$ so that the *sign* of $\omega(k)$ (for a given value of k) determines whether the perturbation grows or decays. As will become clear below, it is convenient to write the stability function $\omega(k)$ in the form

$$\omega(k) = g(k) - k^2 f(k). \quad (13)$$

Our task now is to determine $\omega(k)$ as a function of the various parameters of the step-flow problem. To do so, it is useful to reexpress all these quantities in terms of characteristic lengths. Therefore, in addition to the terrace width l and the surface diffusion length x_s , we define two kinetic lengths $d_{\pm} = D_s / k_{\pm}$, which express the relative importance of step attachment kinetics to surface diffusion, and a surface capillary length $\xi = \Gamma / \tau(F - F_{\text{eq}})$, which expresses the competition between surface tension and the incident flux as agents for mass transport. The quantity $F_{\text{eq}} = c_{\text{eq}}^0 / \tau$ is the incident (or desorbing) flux of particles when the terraces are in equilibrium with their own bulk vapor.

Now, rather than proceed immediately to the most general situation (which is quite complex) it is instructive to consider first the extreme case where step attachment is infinitely fast from the lower terrace and infinitely slow from the upper terrace ($d_- \rightarrow \infty, d_+ = 0$). Carrying out the steps indicated above for this "one-sided" problem one readily finds that

$$g(k) = \Omega(F - F_{\text{eq}}) \frac{\text{sech}(l/x_s) + x_s \Lambda_k \tanh(l/x_s) \sinh(\Lambda_k l) - \cosh(\Lambda_k l)}{\cosh(\Lambda_k l)} \quad (14)$$

and

$$f(k) = D_s \Omega \Gamma \Lambda_k \tanh(\Lambda_k l). \quad (15)$$

It is easily verified that both $f(k)$ and $g(k)$ are positive definite functions of k . For typical values of the parameters, $\omega(k)$ has the behavior illustrated in Fig. 3. As expected from our qualitative discussion, $\omega(k)$ is positive at long wavelength and negative at short wavelength.

The critical wavelength λ_c is given by $\lambda_c = 2\pi/k_c$,

where k_c is defined by $\omega(k_c) = 0$. Figure 4 illustrates the dependence of this quantity on the surface capillary length ξ for several different values of the terrace width l . Observe that k_c goes to zero abruptly at some critical value ξ_c . Thus, there is a crossover from morphologically unstable step flow ($\xi < \xi_c$) to morphologically stable step flow ($\xi > \xi_c$). This result arises entirely from the fact that the diffusion length x_s is finite and can be understood with a simple amendment to our qualitative argu-

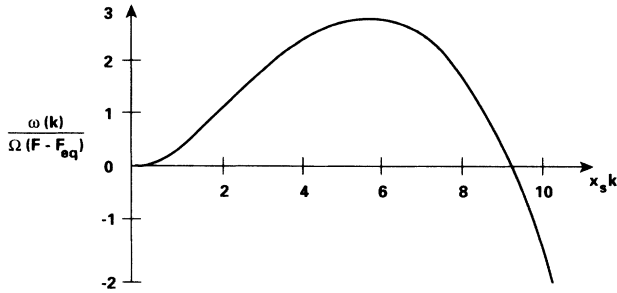


FIG. 3. Plot of the stability function $\omega(k)$ vs perturbation wave vector k for typical values of the model parameters.

ment. In short, since x_s sets the range of the diffusion field (along the step), desorption can short circuit the communication needed to drive a diffusive instability at the longest wavelengths. As $x_s \rightarrow \infty$, unstable step flow persists at long wavelength for any value of ξ . Complimentary information can be gleaned from a plot of k_c versus terrace width for various values of the capillary length (Fig. 5). Note that k_c saturates for large values of l but cuts off at some smaller value which depends upon the deposition conditions. In this case, the terrace width itself limits the action of the diffusion field.

Analytic expressions for k_c can be found from Eq. (13) in the limit of both very large and very small terrace widths. For example, when $l \gg x_s$, we find

$$x_s k_c = \left[\left(\frac{x_s}{\xi} \right)^{1/2} \right], \quad x_s k_c \gg 1 \tag{16a}$$

$$x_s k_c = \left[\frac{4}{3} \left[1 - 2 \frac{\xi}{x_s} \right] \right]^{1/2}, \quad x_s k_c \ll 1 \tag{16b}$$

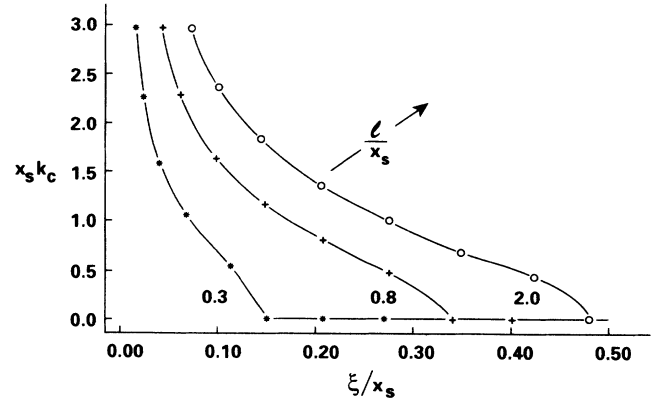


FIG. 4. Plot of the variation of the critical wave vector k_c vs the surface capillary length ξ for various values of the terrace width l .

for the asymptotic values of k_c . Since k_c must be real, we obtain the condition $\xi < \xi_c = x_s/2$ as a prerequisite for morphological instability. Similarly, when $l \ll x_s$ (and $l^2 \ll \lambda_c^2$) it is easy to show that

$$x_s k_c = \left[\frac{l}{2\xi} - 1 \right]^{1/2}. \tag{17}$$

The cutoff is now $\xi_c = l/2$, illustrating that the quantities x_s and l have exchanged roles as the limiting factors to morphological instability.³⁶

We now turn to the general case where d_+ and d_- are both finite. After a heroic bout of algebra, one finds that

$$f(k) = \frac{2D_s \Omega \Gamma \Lambda_k \cosh(\Lambda_k l) + \Lambda_k^2 (d_+ + d_-) \sinh(\Lambda_k l)}{\Lambda_k (d_+ + d_-) \cosh(\Lambda_k l) + [d_+ d_- \Lambda_k^2 + 1] \sinh(\Lambda_k l)} \tag{18}$$

and

$$g(k) = \Omega (F - F_{eq}) (d_- - d_+) \mathcal{G}(k), \tag{19}$$

where

$$\mathcal{G}(k) = \frac{\Lambda_k (d_+ + d_-) [\text{sech}(l/x_s) + \Lambda_k x_s \sinh(\Lambda_k l) \tanh(l/x_s) - \cosh(\Lambda_k l)]}{\{(d_+ + d_-) + [(d_+ d_- / x_s) + x_s] \tanh(l/x_s)\} [\Lambda_k (d_+ + d_-) \cosh(\Lambda_k l) + (d_+ d_- + \Lambda_k^2 + 1) \sinh(\Lambda_k l)]} + \frac{[1 - (x_s \Lambda_k)^2] [\text{sech}(l/x_s) - 1] \sinh(\Lambda_k l)}{\{(d_+ + d_-) + [(d_+ d_- / x_s) + x_s] \tanh(l/x_s)\} [\Lambda_k (d_+ + d_-) \cosh(\Lambda_k l) + (d_+ d_- + \Lambda_k^2 + 1) \sinh(\Lambda_k l)]}. \tag{20}$$

The function $f(k)$ is still positive definite and thus, from Eq. (13), always favors stability. This is to be expected since this term arises entirely from the Gibbs-Thomson effect. Although less obvious, the function $\mathcal{G}(k)$ is also positive definite. Thus step flow is absolutely stable if $d_+ > d_-$. Conversely, if $d_+ < d_-$, morphologically unstable step flow occurs so long as the capillary length $\xi < \xi_c$. We solve for the critical value ξ_c by expanding

the equation $\omega(k_c) = 0$ for small k_c and requiring k_c to be real. The result is

$$\xi_c = \frac{\frac{1}{2} x_s^2 (d_- - d_+)}{x_s (d_- + d_+) \coth(l/x_s) + d_- d_+ + x_s^2}. \tag{21}$$

As expected, the critical value is zero when $d_+ = d_-$ and the step is always stable.

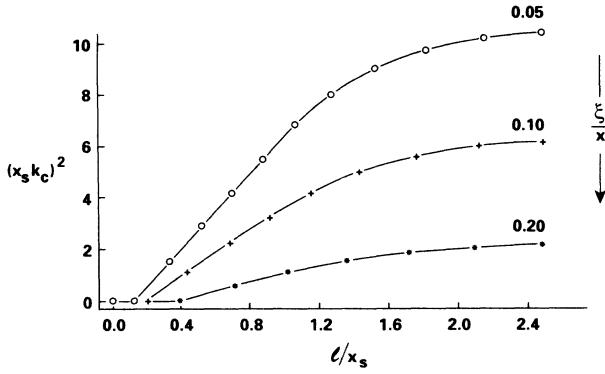


FIG. 5. Plot of the variation of the critical wave vector k_c vs the terrace with l for various values of the surface capillary length ξ .

The principal effect of finite step attachment kinetics is to push the terrace edge instability to longer wavelength. This is in agreement with known results for the conventional Mullins-Sekerka problem.³⁷ In particular, the dependence of the critical wave number on l and ξ remains very similar to that illustrated in Figs. 4 and 5 except that the value of k_c is systematically reduced. This can be seen analytically most easily for the special case of upper terrace blocking ($d_- \rightarrow \infty$) examined earlier. Thus, for the asymptotic values of k_c one now has in place of Eqs. (16) and (17):

$$x_s k_c = \begin{cases} \left[\frac{x_s/\xi}{1+d_+/x_s} \right]^{1/2}, & x_s k_c \gg 1 \\ \left[\frac{4}{3} \left[1 - 2 \frac{\xi}{x_s} \left[1 + \frac{d_+}{x_s} \right] \right] \right]^{1/2}, & x_s k_c \ll 1, \end{cases} \quad (22a)$$

(22b)

when $l \gg x_s$ and

$$x_s k_c = \left[\frac{l/2\xi}{1+ld_+/x_s^2} - 1 \right]^{1/2} \quad (23)$$

when $l \ll x_s$.

This concludes our quantitative treatment of morphological instability during step flow. However, as noted in the Introduction, layer growth also can occur via the nucleation and spread of two-dimensional islands. Quite apart from reasons related to reduced adatom mobility, this will occur whenever the adatom supersaturation on the terraces, $\sigma(\mathbf{r}) = [c(\mathbf{r}) - c_{\text{eq}}^0]/c_{\text{eq}}^0$, exceeds some critical value σ_n computable from the standard theory of heterogeneous nucleation.^{13,38} Since, for our problem, the adatom concentration is computed from Eq. (1), it is more convenient to speak in terms of a critical flux or, better still, a critical capillary length for nucleation, ξ_n . Clearly, ξ_n depends upon all the remaining characteristic length parameters because $\sigma(\mathbf{r})$ does so itself. The exact functional form turns out to be

$$\xi_n = \xi_n^\infty [1 - \Xi(l, x_s, d_\pm)], \quad (24)$$

where

$$\Xi(l, x_s, d_\pm) = \frac{x_s \sqrt{\{(d_- - x_s)[\cosh(l/x_s) - \sinh(l/x_s)] + d_+ + x_s\} \{(d_- + x_s)[\cosh(l/x_s) + \sinh(l/x_s)] + d_+ - x_s\}}}{x_s(d_- + d_+) \cosh(l/x_s) + (d_- d_+ + x_s^2) \sinh(l/x_s)} \quad (25)$$

and ξ_n^∞ is computed from the critical supersaturation for nucleation on an infinitely large terrace.^{13,38} We hasten to add that the exact value of ξ_n^∞ is somewhat arbitrary since growth can proceed by nucleation and step flow simultaneously.³⁹ Indeed, one easily can imagine a nucleated island whose perimeter becomes unstable as it spreads.

All of our results can best be summarized by means of a morphological phase diagram which separates regions of stable step flow, unstable step flow, and 2D nucleation (Fig. 6). The boundary between step flow and 2D nucleation is given by the curve ξ_n/ξ_c^∞ while the boundary between stable and unstable step flow is given by the curve ξ_c/ξ_c^∞ . The quantity ξ_c^∞ is the critical capillary length for a wide ($l \gg x_s$) terrace given by Eq. (21) as

$$\xi_c^\infty = \frac{x_s^2(d_- - d_+)}{2[x_s(d_- + d_+) + d_- d_+ + x_s^2]}. \quad (26)$$

The precise appearance of the diagram depends on the kinetic parameters d_\pm and the value of ξ_n^∞ . For example,

in Fig. 6, one can pass from stable step flow to unstable step flow to 2D nucleation simply by progressively increasing the deposition rate. It is possible, however, that $\xi_n > \xi_c$ for all l . In such a situation, 2D nucleation takes over as the dominant growth mechanism before any step can become unstable.

IV. DISCUSSION

The preceding section illustrated that an infinitesimal shape perturbation to a (nominally) straight terrace edge will not be damped during step flow if the kinetics of adatom attachment are sufficiently asymmetric. It remains to examine the limitations of this analysis and discuss how the instability might be observed under actual epitaxial growth conditions. There are three outstanding issues: the effect of crystalline *anisotropy* in D_s , γ , and k_\pm , the predicted shape of the terrace edges as the perturbation amplitude increases beyond the range of validity of the linear stability analysis, and the effect of step-step interactions. We deal with each of these in turn.

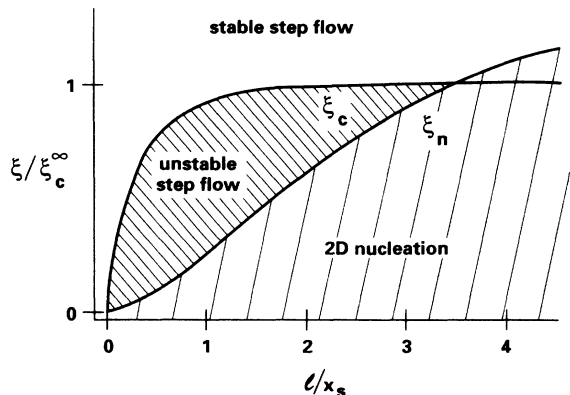


FIG. 6. Morphological phase diagram for crystal growth on a vicinal surface as a function of terrace width l (miscut) and surface capillary length ξ (inverse deposition rate).

The anisotropy of surface diffusion coefficients is a well-established experimental fact. In the present context, anisotropic Ga-atom diffusion on (001) GaAs has been invoked to explain both terrace width ordering⁴⁰ and differences between OMVPE and MBE (Ref. 41) observed during the growth of tilted superlattices. Our results will be altered only slightly if we identify our quantity D_s with the value of surface diffusion in the direction *perpendicular* to the direction of step flow. If the value of the surface diffusion along the direction of step flow differs, there will be some quantitative change in, e.g., the mean velocity of the steps and those quantities that directly involve the ratio l/x_s . There are no qualitative changes.

The free energy (surface tension) γ enters our problem only through the Gibbs-Thomson relation, Eq. (3). Throughout, we have treated this quantity as a constant. In fact, one should write $\gamma(dz/dx)$ [cf. Eq. (9)], to reflect the fact that the terrace edge free energy generally depends upon the orientation of the step in the z - x plane (Fig. 1). This is important because significant anisotropy can exist even if one is (as we assume) well above the step roughening temperature.²⁵ The appropriate generalization of the Gibbs-Thomson relation to this case is known as Herring's equation⁴² and its effect on perturbation analyses similar to the one we have performed is well known.^{32,43} Above T_R , we need only make the replacement $\gamma \rightarrow \gamma + \gamma_{xx}$, where γ_{xx} is the coefficient of the second-order term in a Taylor expansion of $\gamma(dz/dx)$ around $dz/dx = 0$. This change enters our results by altering the magnitude of the quantity Γ [Eq. (3)] and therefore both ξ and the function $f(k)$ [Eqs. (15) and (18)]. Two extreme cases make clear the morphological consequences.

Suppose first that $\gamma(dz/dx)$ has a local minimum at $dz/dx = 0$, i.e., the unperturbed terrace edge would be a one-dimensional *facet* if $T < T_R$. In that case, $\gamma_{xx} > 0$ and its magnitude easily can exceed that of γ itself, even for relatively weak anisotropy. The net effect is to reduce the tendency towards instability by shifting the critical wavelength to larger values [Eq. (13)]. This is clear from the expressions for k_c in, e.g., Eqs. (16) and (17). Con-

versely, if $\gamma(dz/dx)$ exhibits a local *maximum* when $dz/dx = 0$, $\gamma_{xx} < 0$, and the tendency toward instability is enhanced. In fact, it is clear that the linear instability we predict ultimately must evolve to a "hill-and-valley" facet structure in analogy with Herring's discussion⁴⁴ of spontaneous faceting at a free surface.

At the level of linear stability theory, the treatment of anisotropic attachment kinetics [$d_{\pm}(dz/dx)$] proceeds identically to the foregoing case of anisotropic surface tension. Indeed, apart from the fact that sinusoidal shape perturbations are translated parallel to the unperturbed step as they increase in amplitude,⁴³ the qualitative results are unchanged as well because the crystallographic dependence of $d_{\pm}(dz/dx)$ is expected to be quite similar to that of $\gamma(dz/dx)$.⁴⁵

This brings us naturally to the question of what one should see in, e.g., an electron or scanning tunneling microscope, if the experimental growth conditions favor terrace edge instability. Based upon our linear analysis, one might expect to observe step edges modulated sinusoidally at a wavelength λ_{\max} corresponding to the wave vector $k_{\max} < k_c$, where $\omega(k)$ (Fig. 3) has its maximum. As it happens, this is unlikely to be the case because an advancing terrace edge very rapidly passes out of the small amplitude perturbation limit and enters a regime of nonlinear morphological evolution which strongly mixes individual Fourier modes. This expectation is based upon experience gained in the study of directional solidification⁴⁶ (a closely related problem which also exhibits a Mullins-Sekerka instability) where a distinct cellular morphology is observed at all times. Unfortunately, precise theoretical prediction of the final interfacial pattern that evolves from a particular linear instability is a difficult and incompletely solved problem.⁴⁷

Moreover, step flow involves an additional complication. Our linear stability analysis neglects any possible interactions between terrace edges. In fact, such interactions exist; most notably, a dipolar repulsion between adjacent steps arising from entropic and elasticity considerations.⁴⁸ If no other processes intervene, these forces are sufficient to drive the motion of steps across a vicinal surface.⁴⁹ In the presence of a deposition flux, the qualitative effect is to keep terrace edges from getting too close together and thus to limit the growth of step waviness. However, this effect is likely to be most noticeable only when the meanderings of the steps approach substantial fractions of the terrace width itself. This is the regime of highly nonlinear evolution—to which we now return.

With the foregoing caveat in mind, and as a guide to the experimentalist, we now draw upon the analogy to the well-studied problem of pattern formation during solidification from the melt⁵⁰ to make some reasonable guesses as to how a well-developed terrace edge instability might manifest itself. For the planar geometry of interest here, detailed studies exist only for the one-sided situation referred to here as upper terrace blocking ($d_- \rightarrow \infty$). In a somewhat different context, we ourselves have dealt with this problem⁵¹ for the case of isotropic surface tension and isotropic attachment kinetics. When the kinetics are very fast ($d_+ = 0$) so that the growth is

diffusion limited, one obtains a distinctive fingerlike morphology where (at least for early times) the spacing between fingers is very nearly equal to the quantity λ_{\max} defined above. By contrast, when the kinetics are rather slow, the interface quickly develops a "scalloped" morphology formed from a sequence of outward bulging parabolic arcs which spread laterally and compete with one another. This process continues until the scallops reach a limiting width ($\sim d_+$), whereupon further evolution again results in a fingerlike morphology.

One-sided directional solidification has been studied in the weakly nonlinear regime by bifurcation theory for the cases of both anisotropic surface tension⁵² and anisotropic kinetics.^{53,54} One finds significant modifications to the basic cellular morphology obtained in the isotropic case (for that problem) so that a similar analysis for the present problem appears warranted. Otherwise, it is generally understood that diffusion limited growth in the presence of anisotropic surface tension can produce dendritic structures.^{47,55} Hence, "surface dendrites" might be observable during step flow under suitable conditions. Similarly, when anisotropic attachment kinetics dominate, a stable macrostep morphology has been predicted⁵⁶ for the case of solution growth. This would appear as a propagating "ragged" terrace edge for our problem. To our knowledge, nothing is known for the case when anisotropic surface tension and anisotropic kinetics compete on an equal footing. And finally, to reiterate, we have no explicit morphological prediction for the real step-flow problem for the (most) realistic case when both d_- and d_+ are finite.

This leads us to a difficult point. The reader will have noticed that we have not attempted to numerically estimate any of the key parameters of our theory that would aid an experimental search. A good candidate would be λ_{\max} . In fact, all of the key ingredients *can* be estimated—except one: the difference $d_+ - d_-$, or equivalently, $k_+ - k_-$. Unfortunately, almost nothing is known about the magnitude of step attachment coefficients, even in the symmetric case,⁵⁷ much less their difference. Moreover, since both are activated, the difference easily can range over several orders of magnitude. This uncertainty, plus a similar lack of knowledge about the magnitude of γ_{xx} , leads to estimates of λ_{\max} that range from a few Å to hundreds of micrometers. We

are unable to be more precise.

Finally, given the foregoing, it is worth asking how one can distinguish the wavy step patterns we predict from the waviness associated with thermal roughening. In both cases, increased temperature increases the irregularity of terrace edges. The key difference lies in the dependence upon deposition flux. We expect a large effect for the instability discussed here (Fig. 6), while no great changes are expected for the case of thermal wandering. Moreover, true thermal roughening exhibits a special signature in scattering experiments⁵⁸ which is unlikely to be mimicked by a diffusional instability studied by, say, a RHEED spot profile analysis.⁵⁹

V. CONCLUSION

In this paper we have considered the possibility that monoatomic terrace edges undergo a morphological instability during epitaxial step-flow growth. Linear stability theory predicts that such an instability can occur *only* when the energy barriers to adatom attachment to steps *differ* for adatoms that approach a step from *opposite* directions. This condition turns out to be the usual physical situation. The instability is diffusional in origin and manifests itself as a distinct waviness or meandering of the terrace edges as they propagate across the crystal. The basic physics of the instability is qualitatively similar to the physics of dendritic growth.

Our results, presented in the form of a morphological phase diagram, show that single-crystal growth on a vicinal surface can pass from stable step flow to unstable step flow to 2D island nucleation and spreading as one increases the incident flux in, say, a molecular-beam-epitaxy experiment. We have discussed qualitatively how our results are affected if one takes account of certain complicating factors neglected in our quantitative analysis. Although no numerical estimates were given, the terrace edge instability we predict should be readily distinguishable from simple thermal fluctuations.

ACKNOWLEDGMENTS

The authors gratefully acknowledge support for this work under U.S. Department of Energy Grant No. DE-FG05-88ER45369.

¹See the various contributions to MRS Bull. **13**, No. 11 (1988).

²See, for example, E. G. Bauer, J. Mater. Res. (to be published).

This article is a U.S. Department of Energy Panel Report on "Fundamental Issues in Heteroepitaxy."

³F. Rosenberger, in *Interfacial Aspects of Phase Transformations*, edited by B. Mutaftschiev (Reidel, Dordrecht, 1982), pp. 315–364.

⁴H. Asai, J. Cryst. Growth **80**, 425 (1987).

⁵A. J. Hoeven, J. M. Lensicnck, D. Dijkkamp, E. J. van Loenen, and J. Dieleman, Phys. Rev. Lett. **63**, 1830 (1989).

⁶See the various contributions to *Reflection High Energy Electron Diffraction and Reflection Electron Imaging of Surfaces*, edited by P. K. Larsen and P. J. Dobson (Plenum, New York, 1988).

⁷J. H. Neave, P. J. Dobson, B. A. Joyce, and J. Zhang, Appl. Phys. Lett. **47**, 100 (1985).

⁸A. A. Chernov, *Modern Crystallography III* (Springer-Verlag, Berlin, 1984).

⁹M. Mundschaue, E. Bauer, W. Teliemps, and W. Swiech, Surf. Sci. **213**, 381 (1989).

¹⁰J. M. Gaines, P. M. Petroff, H. Kroemer, R. J. Simes, R. S. Geels, and J. H. English, J. Vac. Sci. Technol. B **6**, 1378 (1988).

¹¹M. Tanaka and H. Sakaki, Jpn. J. Appl. Phys. Pt. 2 **27**, L2025 (1988).

¹²C. P. Flynn, J. Phys. F **18**, L195 (1988).

¹³T. Nishinaga and K. I. Cho, Jpn. J. Appl. Phys. Pt. 2 **27**, L12 (1988).

- ¹⁴W. K. Burton, N. Cabrera, and F. C. Frank, *Philos. Trans. R. Soc. London, Ser. A* **243**, 299 (1951).
- ¹⁵P. Bennema and G. H. Gilmer, in *Crystal Growth, An Introduction*, edited by P. Hartmann (North-Holland, Amsterdam, 1973), pp. 263–327.
- ¹⁶R. L. Schwoebel, *J. Appl. Phys.* **40**, 614 (1969).
- ¹⁷R. Ghez and S. S. Iyer, *IBM J. Res. Develop.* **32**, 804 (1988).
- ¹⁸H. Hoche and H. Bethge, *J. Cryst. Growth* **52**, 27 (1981).
- ¹⁹B. van der Hoek, J. P. van der Eerden, and P. Bennema, *J. Cryst. Growth* **56**, 108 (1982).
- ²⁰H. C. Abbink, R. M. Broudy, and G. P. McCarthy, *J. Appl. Phys.* **39**, 4673 (1968).
- ²¹I. Sunagawa and P. Bennema, in *Preparation and Properties of Solid State Materials*, edited by W. R. Wilcox (Dekker, New York, 1982), Vol. 7, pp. 1–129.
- ²²P. R. Pukite, G. S. Petrich, S. Batra, and P. I. Cohen, *J. Cryst. Growth* **95**, 269 (1989).
- ²³R. T. Tung and F. Schrey, *Phys. Rev. Lett.* **63**, 1277 (1989).
- ²⁴C. van Leeuwen and F. H. Mischgofsky, *J. Appl. Phys.* **46**, 1056 (1975).
- ²⁵H. J. Leamy, G. H. Gilmer, and K. A. Jackson, in *Surface Physics of Materials*, edited by J. M. Blakely (Academic, New York, 1975), Vol. 1, pp. 121–188.
- ²⁶V. V. Voronkov, in *Modern Theory of Crystal Growth I*, edited by A. A. Chernov and H. Muller-Krumbhaar (Springer-Verlag, Berlin, 1983), pp. 75–111.
- ²⁷H. van Beijeren and I. Nolden, in *Structure and Dynamics of Surfaces II*, edited by W. Schommers and P. von Blanckenhagen (Springer-Verlag, Berlin, 1987), pp. 259–300.
- ²⁸R. F. Sekerka, in *Crystal Growth, an Introduction*, edited by P. Hartmann (North-Holland, Amsterdam, 1973), pp. 403–443. See also C. H. J. van den Brekel and A. K. Jansen, *J. Cryst. Growth* **43**, 364 (1978) for an analysis that employs a notation similar to that of the present paper.
- ²⁹The diffusive transport in the vapor phase which characterizes chemical-vapor deposition leads to morphological complications we choose to avoid. For some discussion of this point, see C. Ratsch, G. S. Bales, and A. Zangwill (unpublished) for the case of layer growth during OMVPE.
- ³⁰Formally, one should work in a frame of reference moving with the velocity V of the steps. This introduces a “convection” term into Eq. (1). With BCF, we suppose that $V \ll \sqrt{D_s/\tau}$ so that this term may be neglected. See Ref. 17 for a BCF-type analysis taking this effect into account.
- ³¹This effect occurs for the same reason that the electric field is very large at the tip of a lightning rod. See, e.g., J. D. Jackson, *Classical Electrodynamics*, 2nd ed. (Wiley, New York, 1975), pp. 75–78.
- ³²W. W. Mullins, in *Metal Surfaces: Structure, Energetics and Kinetics*, edited by W. D. Robertson and N. A. Gjostein (Metall. Soc. AIME, Metals Park, Warrendale, PA, 1963), pp. 17–66.
- ³³L. D. Landau and E. M. Lifshitz, *Statistical Physics* (Addison-Wesley, Reading, MA, 1969), Chap. 15.
- ³⁴H.-W. Fink and G. Ehrlich, *Surf. Sci.* **173**, 128 (1986).
- ³⁵M. Tsuchiya, P. M. Petroff, and L. A. Coldren, *Appl. Phys. Lett.* **54**, 1690 (1989).
- ³⁶The factors of 2 in the expressions for ξ_c arise from the non-standard definition of the diffusion length adopted by BCF. They disappear if, as is more conventional, one defines $x_c^2 = 2D_s\tau$ for diffusion in two dimensions. See, e.g., A. Zangwill, *Physics at Surfaces* (Cambridge University Press, Cambridge, 1988), p. 375.
- ³⁷P. G. Shewmon, *Trans. Metall. Soc. AIME* **233**, 736 (1965).
- ³⁸J. P. Hirth and G. M. Pound, *Condensation and Evaporation* (Macmillan, New York, 1963), pp. 87–90.
- ³⁹S. Clarke and D. D. Vvedensky, *J. Appl. Phys.* **63**, 2272 (1988).
- ⁴⁰Y. Tokura, H. Saito, and T. Fukui, *J. Cryst. Growth* **94**, 46 (1989).
- ⁴¹M. Kawabe and T. Sugaya, *Jpn. J. Appl. Phys. Pt. 2* **28**, L1077 (1989).
- ⁴²C. Herring, in *The Physics of Powder Metallurgy*, edited by W. E. Kingston (McGraw-Hill, New York, 1951), pp. 143–179.
- ⁴³S. R. Coriell and R. F. Sekerka, *J. Cryst. Growth* **34**, 157 (1976).
- ⁴⁴C. Herring, *Phys. Rev.* **82**, 87 (1951).
- ⁴⁵A. A. Chernov and T. Nishinaga, in *Morphology of Crystals*, edited by I. Sunagawa (Terra, Tokyo, 1987), Pt. A, pp. 207–267.
- ⁴⁶S. R. Coriell, G. B. McFadden, and R. F. Sekerka, *Annu. Rev. Mater. Sci.* **15**, 119 (1985).
- ⁴⁷D. A. Kessler, J. Koplik, and H. Levine, *Adv. Phys.* **37**, 255 (1988).
- ⁴⁸A. F. Andreev and Yu. A. Kosevich, *Zh. Eksp. Teor. Fiz.* **81**, 1435 (1981) [*Sov. Phys.—JETP* **54**, 761 (1981)]; E. E. Gruber and W. W. Mullins, *J. Phys. Chem. Solids* **28**, 875 (1967).
- ⁴⁹G. Martin and B. Perrailon, *Surf. Sci.* **68**, 57 (1977).
- ⁵⁰J. S. Langer, *Rev. Mod. Phys.* **52**, 1 (1980).
- ⁵¹G. S. Bales, A. C. Redfield, and A. Zangwill, *Phys. Rev. Lett.* **62**, 776 (1989).
- ⁵²G. B. McFadden, S. R. Coriell, and R. F. Sekerka, *J. Cryst. Growth* **91**, 180 (1988).
- ⁵³G. W. Young, S. H. Davis, and K. Brattkus, *J. Cryst. Growth* **83**, 560 (1987).
- ⁵⁴E. N. Kolesnikova and V. S. Yuferev, *Kristallografiya* **34**, 16 (1989) [*Sov. Phys.—Crystallogr.* **34**, 7 (1989)].
- ⁵⁵R.-F. Xiao, J. I. D. Alexander, and F. Rosenberger, *Phys. Rev. A* **38**, 2447 (1988).
- ⁵⁶V. V. Voronkov, in *Growth of Crystals*, edited by E. I. Givargizov (Consultants Bureau, New York, 1986), Vol. 13, pp. 127–136.
- ⁵⁷A. A. Chernov, L. N. Rashkovich, I. L. Smol'skii, Yu. G. Kuznetsov, A. A. Mkrtychyan, and A. I. Malkin, in *Growth of Crystals*, edited by E. I. Givargizov and S. A. Grinberg (Consultants Bureau, New York, 1988), Vol. 15, pp. 43–91; M. Klava, in *Growth of Crystals*, edited by A. A. Chernov and J. E. S. Bradley (Consultants Bureau, New York, 1979), Vol. 11, pp. 60–63.
- ⁵⁸B. Salanon, F. Fabre, J. Lapujoulade, and W. Selke, *Phys. Rev. B* **38**, 7385 (1988).
- ⁵⁹D. Saloner, J. A. Martin, M. C. Tringides, D. E. Savage, C. E. Aumann, and M. G. Lagally, *J. Appl. Phys.* **61**, 2884 (1987).